ELSEVIER

S0032-3861(96)00234-0

Polymer Vol. 37 No. 18, pp. 4003–4008, 1996

0032-3861/96/$15.00 + 0.00

polymer papers

Biparabolic model to represent dielectric relaxation data

R. Diaz-Calleja* and M. J. Sanchis
Departamento Termodinámica Aplicada, Universidad Politécnica de Valencia, València E-46071, Spain

and J. Mostos
Matemática Aplicada, Universidad Politécnica de Valencia, València E-46071, Spain
(Received 5 May 1994; revised 6 April 1995)

The expression of a biparabolic model to represent the dielectric relaxation data of polymers is combined with a statistical method (the LEVM6 program) to provide a reasonable estimation of the parameters of this model. The graphical and multi-response methods are compared by using data for poly(2,6-dimethylphenyl methacrylate) (PDMP). The statistical techniques lead to a much quicker, objective estimation of parameters and also permits a sensitive analysis of the residuals. Copyright © 1996 Elsevier Science Ltd.

(Keywords: dielectric relaxation; biparabolic model; statistical analysis)

INTRODUCTION

The success of the model proposed by Havriliak and Negami to represent the dielectric data in primary or secondary relaxation zones is already well known[1,2]. The flexibility provided by the five parameters of this equation allows us to fit much of the experimental data. On the other hand, the Cole–Cole[3] and the Davidson–Cole[4] equations are particular cases of the Havriliak–Negami (H–N) equation. Recently, Schonhals and Schlosser[5–7] proposed a physical interpretation of the two exponents appearing in the H–N equation. At about the same time that the H–N equation was proposed, Huet proposed a representation of the viscoelastic properties of some bituminous asphalts by means of a biparabolic model[8]:

$$E^* = E_0 + \frac{E_\infty - E_0}{1 + \delta(j\omega\tau_0)^{-k} + (j\omega\tau_0)^{-h}} \qquad (1)$$

where E_0 and E_∞ represent the relaxed and unrelaxed moduli, respectively, τ_0 is the relaxation time and δ, h, and k are parameters, where $1 > h > k > 0$. The name of this model corresponds to the geometric shape of the creep function t^{-k}, whose Laplace transform is proportional to $(j\omega\tau_0)^{k-1}$ according to the following:

$$\mathscr{L}\left(t^{-k}\right)(j\omega) = A(j\omega\tau_0)^{k-1} \qquad (2)$$

where $A = \Gamma(1-k)/\tau_0^{k-1}$, Γ is the gamma-function and $\mathscr{L}$ is the Laplace transform.

From the point of view of impedance spectroscopy methodology[9], $(j\omega\tau_0)^k$ is a constant phase element (CPE), which can be motivated by fractional differential calculus[10]. This element was first mentioned (historically) by Cole and Cole[3] as an essential ingredient of the semiempirical model corresponding to the dielectric response of a material having a symmetric distribution of relaxation times. Mechanically, a parabolic element contains the spring and dashpot elements as particular cases. From an electrical point of view, it contains a pure resistance or a capacitance as the limiting case.

Pérez[11] modelled the viscoelastic response of a material by using a model based on the annihilation of defects in the matrix of that material. The behaviour is controlled by two relaxation times and the limiting equation formally coincides with equation (1). Thus, in contrast to other models, the biparabolic model and the parameters contained within it, do have a physical meaning.

It is our purpose in this present paper to discuss the compliance or permittivity counterpart of the model represented by equation (1) as a convenient starting point for analysing dielectric relaxation data. In this context, it is important to recognize that the biparabolic model has six parameters instead of the five used in the H–N equation. We also propose an electrical circuit corresponding to the model and whose parameters represent the physical situation in the materials under study. Finally, a closed expression for the relaxation times is obtained, in contrast with the approximations for long and short times given by Decroix and co-workers[12,13]. The biparabolic model is well fitted to some of the experimental data.

EXPERIMENTAL

All of the dielectric data reported in this paper have been obtained by means of a DEA 2970 dielectric analyser from TA Instruments.

* To whom correspondence should be addressed

THEORETICAL BACKGROUND

We will use the symbol M^* instead of E^* for the modulus (viscoelastic as well as dielectric), so equation (1) becomes accordingly:

$$M^* = M_0 + \frac{M_\infty - M_0}{1 + \delta(j\omega\tau_0)^{-k} + (j\omega\tau_0)^{-h}} \tag{3}$$

Taking into account that permittivity (or compliance) is in the inverse of the modulus, we obtain from (3) the following:

$$\epsilon^* = \frac{\epsilon_0\epsilon_\infty\left[1 + \delta(j\omega\tau_0)^{-k} + (j\omega\tau_0)^{-h}\right]}{\epsilon_0 + \epsilon_\infty\left[\delta(j\omega\tau_0)^{-k} + (j\omega\tau_0)^{-h}\right]} \tag{4}$$

where $(j\omega\tau_0)^{-k} = (\omega\tau_0)^{-k}\exp(-kj\pi/2)$, and $(j\omega\tau_0)^{-h} = (\omega\tau_0)^{-h}\exp(-kj\pi/2)$.

In order to describe the properties of the model it is convenient to make some rearrangements in equation (4) to obtain the following:

$$\epsilon^* = \epsilon_\infty + \frac{(\epsilon_0 - \epsilon_\infty)\left[1 + \delta'(j\omega\tau_0')^{h-k}\right]}{\left[1 + \delta'(j\omega\tau_0')^{h-k} + (j\omega\tau_0')^{h}\right]} \tag{5}$$

or alternatively:

$$\epsilon^* = \epsilon_0 - \frac{\epsilon_0 - \epsilon_\infty}{\left[1 + \delta'(j\omega\tau_0')^{-k} + (j\omega\tau_0')^{-h}\right]} \tag{6}$$

where:

$$\delta' = \delta\left(\frac{\epsilon_0}{\epsilon_\infty}\right)^{\frac{k}{h}} - 1 \quad \text{and} \quad \tau_0' = \tau_0\left(\frac{\epsilon_0}{\epsilon_\infty}\right)^{\frac{1}{h}} \tag{7}$$

In this form, the formula presents close similarities with the classical expressions for the permittivity appearing in refs 1–3.

Splitting into real and imaginary parts according to $\epsilon^* = \epsilon' - j\epsilon''$, we have:

$$\epsilon' = \epsilon_\infty + (\epsilon_0 - \epsilon_\infty)\frac{1 + \delta'(\omega\tau_0')^{2h-k}\cos\frac{\pi}{2}k + (\omega\tau_0')^{h}\cos\frac{\pi}{2}h + 2\delta'(\omega\tau_0')^{h-k}\cos\frac{\pi}{2}(h-k) + \delta'^{2}(\omega\tau_0')^{2(h-k)}}{1 + 2\left[\delta'(\omega\tau_0')^{h-k}\cos\frac{\pi}{2}(h-k) + (\omega\tau_0')^{h}\cos\frac{\pi}{2}h + \delta'(\omega\tau_0')^{2h-k}\cos\frac{\pi}{2}k\right] + \delta'^{2}(\omega\tau_0')^{2(h-k)} + (\omega\tau_0')^{2h}} \tag{7a}$$

and

$$\epsilon'' = (\epsilon_0 - \epsilon_\infty)\frac{\delta'(\omega\tau_0')^{2h-k}\operatorname{sen}\frac{\pi}{2}k + (\omega\tau_0')^{h}\operatorname{sen}\frac{\pi}{2}h}{1 + 2\left[\delta'(\omega\tau_0')^{h-k}\cos\frac{\pi}{2}(h-k) + (\omega\tau_0')^{h}\cos\frac{\pi}{2}h + \delta'(\omega\tau_0')^{2h-k}\cos\frac{\pi}{2}k\right] + \delta'^{2}(\omega\tau_0')^{2(h-k)} + (\omega\tau_0')^{2h}} \tag{7b}$$

and consequently:

$$\tan\Psi = \frac{\epsilon''}{\epsilon' - \epsilon_\infty} = \frac{\delta'(\omega\tau_0')^{2h-k}\operatorname{sen}\frac{\pi}{2}k + (\omega\tau_0')^{h}\operatorname{sen}\frac{\pi}{2}h}{1 + \delta'(\omega\tau_0')^{2h-k}\cos\frac{\pi}{2}k + (\omega\tau_0')^{h}\cos\frac{\pi}{2}h + 2\delta'(\omega\tau_0')^{h-k}\cos\frac{\pi}{2}(h-k) + \delta'^{2}(\omega\tau_0')^{2(h-k)}} \tag{8a}$$

$$\tan\phi = \frac{\epsilon''}{\epsilon' - \epsilon_0} = -\frac{\delta'(\omega\tau_0')^{h-k}\operatorname{sen}\frac{\pi}{2}k + \operatorname{sen}\frac{\pi}{2}h}{(\omega\tau_0')^{h} + \delta'(\omega\tau_0')^{h-k}\cos\frac{\pi}{2}k + \cos\frac{\pi}{2}h} \tag{8b}$$

from which we can easily obtain the behaviour of the arc for low and high frequencies:

$$\omega \xrightarrow{\lim} \infty \tan\Psi = \tan\frac{\pi}{2k} \quad \rightarrow \lim \omega \xrightarrow{\Psi} \infty = \frac{\pi}{2}k \tag{9a}$$

and

$$\omega \xrightarrow{\lim} 0 \tan\phi = -\tan\frac{\pi}{2}h \quad \rightarrow \lim \omega \xrightarrow{\phi} 0 = -\frac{\pi}{2}h \tag{9b}$$

In the same way for the characteristic retardation time, for which $\omega\tau_0' = 1$, we have:

$$\Psi' = \arctan\left[\frac{\delta'\operatorname{sen}\frac{\pi}{2}k + \operatorname{sen}\frac{\pi}{2}h}{1 + \delta'\cos\frac{\pi}{2}k + \cos\frac{\pi}{2}h + 2\delta'\cos\pi/z(h-k) + \delta'^{2}}\right] \tag{10a}$$

and

$$\phi' = \arctan\left(-\frac{\delta'\operatorname{sen}\frac{\pi}{2}k + \operatorname{sen}\frac{\pi}{2}h}{1 + \delta'\cos\frac{\pi}{2}k + \cos\frac{\pi}{2}h}\right) \tag{10b}$$

To calculate the δ' and τ_0' parameters, starting with a previous knowledge of h and k, we can follow a very simple geometrical procedure. First, we write the following:

$$\frac{\epsilon^* - \epsilon_\infty}{\epsilon_0 - \epsilon^*} = \delta'(j\omega\tau_0')^{-k} + (j\omega\tau_0')^{-h} \tag{11a}$$

and

$$\left.\frac{\epsilon^* - \epsilon_\infty}{\epsilon_0 - \epsilon^*}\right|_{\omega\tau_0'=1} = \delta' j^{-k} + j^{-h} \tag{11b}$$

with $i^{-k} = \exp(-kj\pi/2)$, and $i^{-h} = \exp(-hj\pi/2)$, and representing the experimental data from the left-hand

side of equation (11a), we can obtain δ' and τ_0' from a plot such as that shown in *Figure 1*, where $\vec{r}$ represents vector j^{-h}, and $\vec{r}\,'$ the vector from the extreme of vector $\vec{r}$ to the curve representing $(\epsilon^* - \epsilon_\infty)/(\epsilon_0 - \epsilon^*)$. Similar results can easily be obtained in terms of the modulus representation. The ϵ_0, ϵ_∞, Ψ, ϕ, Ψ', ϕ' and τ_0' parameters are represented in *Figure 2*.

It is interesting to compare the exponent parameters, h and k, appearing in equation (4), with those of the H–N equation[1,2]:

$$\epsilon^* = \epsilon_\infty + \frac{\epsilon_0 - \epsilon_\infty}{[1 + (j\omega\tau_0)^\alpha]^\beta} \quad (0 < \alpha, \beta \leqslant 1) \tag{12}$$

It is well known that the asymptotic behaviour gives the following:

$$\lim_{\omega \longrightarrow \infty} \arctan \left.\frac{\epsilon''}{\epsilon' - \epsilon_\infty}\right|_{HN} = \alpha\beta \tag{13a}$$

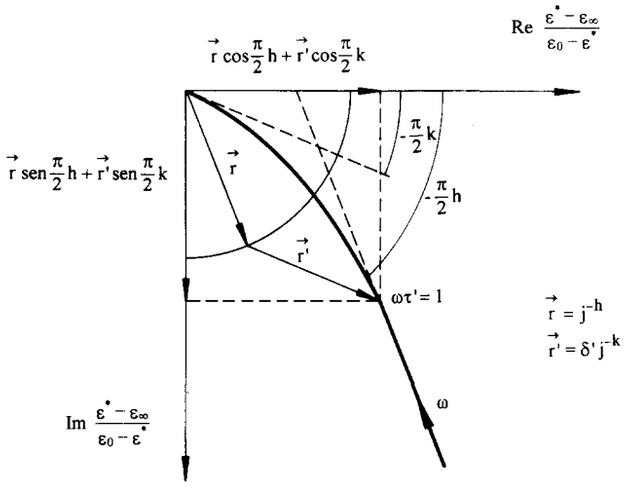

Figure 1 Geometrical calculation of δ

and

$$\lim_{\omega \longrightarrow 0} \arctan \left.\frac{\epsilon''}{\epsilon' - \epsilon_\infty}\right|_{HN} = -\alpha \tag{13b}$$

and comparing these results with equations (9a) and (9b), we obtain:

$$h = \alpha = m$$

$$k = \alpha\beta = n$$

$$\frac{k}{h} = \beta$$

The parameters m and n have been related to the inter- and intramolecular correlations, respectively, i.e. with the long- and short-range molecular motions associated with the relaxation which equation (12) represents[5–7]. Consequently, it is clear that the parameters h and k appearing in equation (4) can be interpreted in a similar way. On the other hand, according to a model proposed by Pérez[14,15], h and k characterize the distribution of activation and diffusion times, respectively, of a defect in a shear microdomain (a mobility island in Johari's terminology)[16] in the polymeric matrix. In this context, it is also interesting to note that the time dependence of these two effects is close to that proposed by Ngai and coworkers in the context of the coupling model[17,18]. Summing up, the lower the values of h and k, then the larger will be the correlation between the species involved in the relaxation. We have shown this effect in recent research on the effect of the static strain on the dynamic mechanical properties of some polyethers[19], the larger the static strain, then the larger the parameters h and k, thus indicating a decrease in correlation in the molecular motion after applying the strain.

ELECTRIC CIRCUIT

In the former section we have seen a way to make a reasonable estimation of the parameters appearing in equation (4). However, in order to find the best set of parameters to fit the experimental data, it would be very convenient to start from all of the experimental points, instead of only from the asymptotic behaviour of the arc,

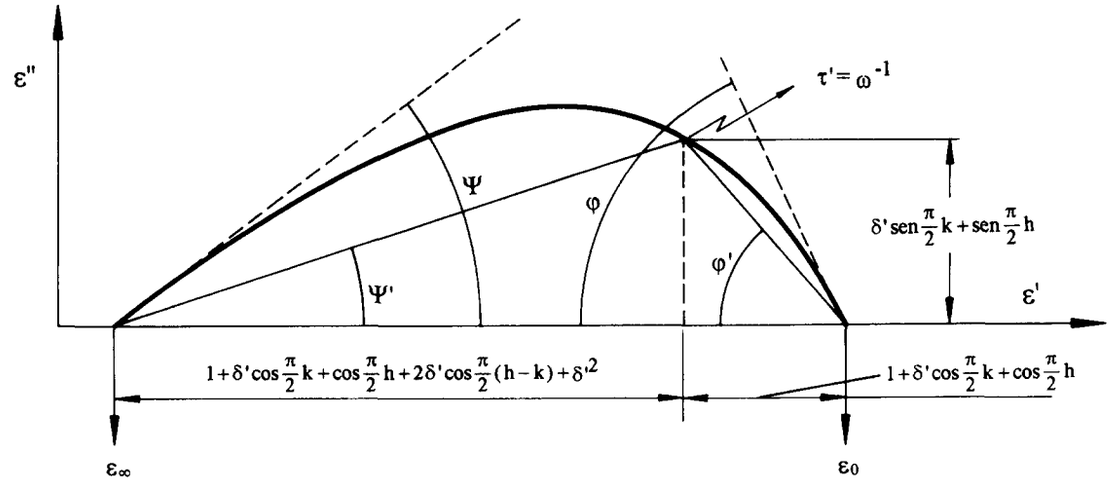

Figure 2 Representation of the Cole–Cole diagram showing the more significant parameters

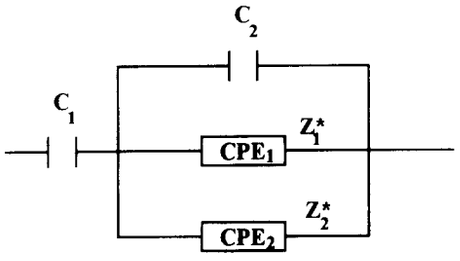

Figure 3 Schematic diagram of the equivalent lump electric circuit

from which only a rough estimation can be obtained. Prior to this, we will synthesize the electric circuit corresponding to the biparabolic model, by following the methodology of impedance spectroscopy analysis. For this purpose we will start from the equation of the biparabolic model in terms of the dielectric modulus, i.e. from equation (3), but taking into account the following:

$$Z^* = \frac{M^*}{j\omega C_0} \tag{15}$$

where C_0 is the capacity of the empty cell; we therefore have the following expression for the equivalent impedance:

$$Z^* = \frac{M_0}{j\omega C_0} + \frac{1}{\frac{j\omega C_0}{\Delta M} + \frac{\delta}{\Delta M} C_0 \tau_0^{-k} (j\omega)^{1-k} + \frac{C_0 \tau_0^{-h}}{\Delta M} (j\omega)^{1-h}} \tag{16}$$

In this way, we have the electric circuit shown in *Figure 3*, where we obtain a capacitance in series with three elements in parallel, where two of these are constant phase elements (CPEs) involving a fractional dependence on the frequency. By comparison of this electric scheme with the biparabolic equation, we have the following:

$$C_1 = C_0 \epsilon_0 \tag{17a}$$

$$C_2 = \frac{\epsilon_0 \epsilon_\infty}{(\epsilon_0 - \epsilon_\infty)} C_0 \tag{17b}$$

$$Z_1^* = \frac{\epsilon_0 - \epsilon_\infty}{\epsilon_0^2 C_0} \frac{\tau_0^{'k}}{\delta'} (j\omega)^{k-1} \tag{17c}$$

and

$$Z_2^* = \frac{\epsilon_0 - \epsilon_\infty}{\epsilon_0^2 C_0} \frac{\tau_0^{'h}}{\delta'} (j\omega)^{h-1} \tag{17d}$$

which relate the parameters of the biparabolic model to the passive elements in the scheme shown in *Figure 3*.

RETARDATION SPECTRUM

A convenient way to represent the relaxation properties of a material is to make use of the distribution of the retardation times, which appears in the linear theory of dielectric relaxation, by means of the following equation:

$$\epsilon^* = \epsilon_\infty + (\epsilon_0 - \epsilon_\infty) \int_0^\infty \frac{\tau g(\tau) d\ln\tau}{1 + j\omega\tau} \tag{18a}$$

where:

$$\int_0^\infty \tau g(\tau) d\ln\tau = 1 \tag{18b}$$

and $g(\tau)$ is the retardation spectrum (sometimes $l(\tau)$ is used instead of $\tau g(\tau)$).

The spectrum can be understood as the number of molecular unities relaxing in a time interval between τ and $\tau + d\tau$; the second equation (18b) is the normalization condition.

Obviously, for a single retardation time, $\tau = \tau_0$, we have:

$$\epsilon^* = \epsilon_\infty + \frac{\epsilon_0 - \epsilon_\infty}{1 + j\omega\tau_0} \tag{19}$$

with the result that the Debye equation is recovered.

The formal expression for $g(\tau)$ depends on the specific model used to represent the empirical data, but in general $g(\tau)$ can be obtained by means of an inversion procedure according to refs 20 and 21:

$$l(\tau) = \tau g(\tau) = \frac{1}{2\pi} \omega \xrightarrow{\lim} 0 [\mathrm{Im}\epsilon^*(-\omega + i/\tau) - \mathrm{Im}\epsilon^*(\omega + i/\tau)] \tag{20}$$

In our case, after several calculations, we obtained the following expression:

$$\tau g(\tau) = \frac{1}{\pi} \left(\frac{\tau}{\tau_0'}\right)^k \frac{\mathrm{sen}h\pi \left(\frac{\tau}{\tau_0'}\right)^{h-k} + \delta' \mathrm{sen}k\pi}{\left(\frac{\tau}{\tau_0'}\right)^{2h} + \delta'^2 \left(\frac{\tau}{\tau_0'}\right)^{2k} + 2\delta' \cos(h-k)\pi \left(\frac{\tau}{\tau_0'}\right)^{h-k} + 2\cos h\pi \left(\frac{\tau}{\tau_0'}\right)^h + 2\delta' \cos k\pi \left(\frac{\tau}{\tau_0'}\right)^k + 1} \tag{21}$$

The distribution functions may, of course, be obtained from the experimental measurements, but we think that it is most interesting to study the changes suffered by this function with respect to the h, k, δ', and τ_0' parameters.

Here, h and k are parameters which describe the low- and high-frequency behaviour, respectively. We can see in *Figure 4a*, that the maximum value of $\tau g(\tau)$ shifts along the abscissa and suffers a progressive diminution to give a minimum at $k \sim 0.25$, which is then followed by the development of a smaller maximum as k is increased further. There are two cases ($k = 0$, $h = k = 0.8$) in which we have a symmetric diagram corresponding to a Cole–Cole expression. In *Figure 4b* we can see that the maximum of the distribution functions decreases and suffers shifts to the left when the h parameter is reduced. Again, when $h = k = 0.4$, we obtain a symmetric Cole–Cole diagram.

When the dependence of $\tau g(\tau)$ on $\ln \tau/\tau_0'$ is studied, the shape distribution function is not altered by the variation of the τ_0' parameter. Finally, we can see in *Figure 4c* the effect of the δ' parameter variation on the distribution of the relaxation times. In this case, the maximum decreases and shifts to the left when the δ' parameter increases. Again, we can see that the symmetric Cole–Cole diagram is obtained if $\delta' = 0$.

APPLICATIONS

In order to study the degree of validity of the parameters (ϵ_0, ϵ_∞, h, k, δ, δ', τ_0, τ_0') obtained by employing the LEVM6 program, as opposed to parameters obtained when using the graphical techniques, we have studied the

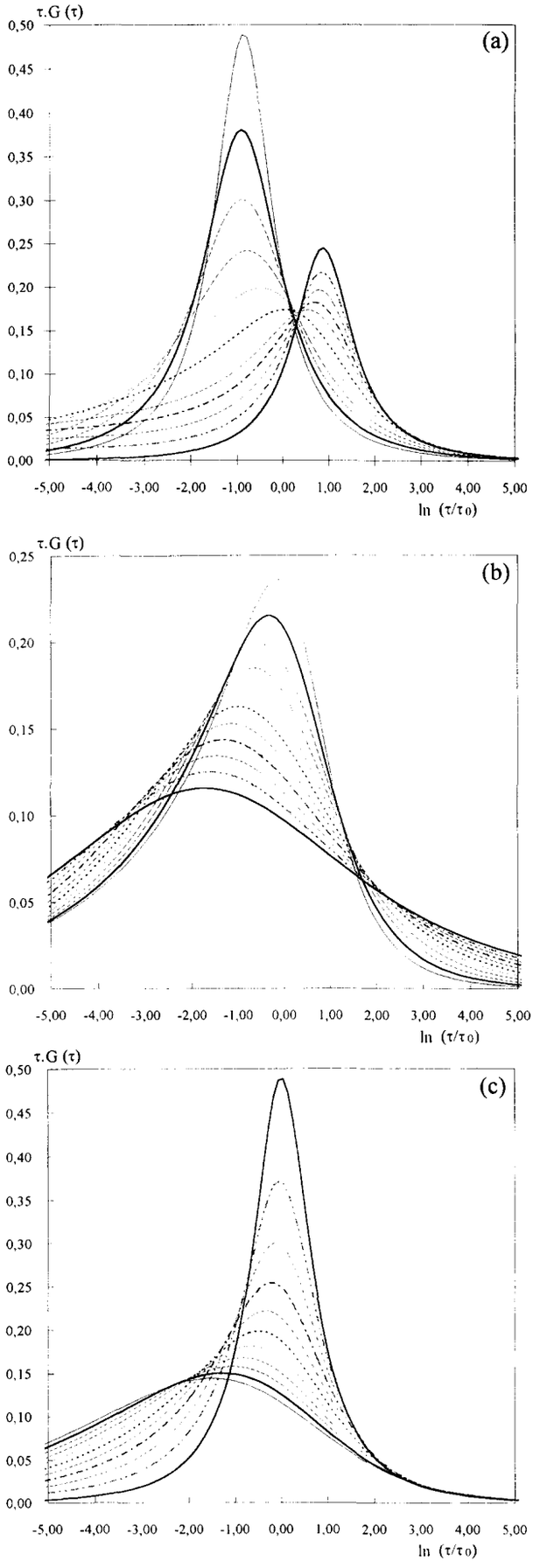

polymer, namely PDMP, which we have reported on recently[22], by using both methods. In *Figure 5* we can see the complex plane representation of the experimental data after the subtraction of the conductive contribution and interfacial relaxation mechanisms caused by the rough contacts of the sample with the electrodes[23].

In *Table 1* we show the best estimates for the parameters obtained from both methods. The first column gives the parameters reported previously, by

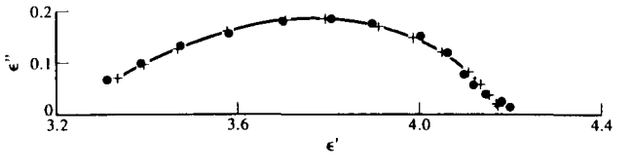

Figure 5 Complex plane representation of PDMP at 195°C: (●) experimental data; (+) estimated values

Table 1 Parameters obtained for PDMP by using the graphical method and the LEVM6 program

Parameter	Graphical method	LEVM6 program
ϵ_0	4.259	4.1854
ϵ_∞	3.093	3.2175
h	0.4950	0.7429
k	0.1950	0.3693
δ	0.650	1.1594
δ'	1.0633	1.5128
τ_0 (s)	1.66×10^{-5}	4.66×10^{-5}
τ_0' (s)	8.56×10^{-5}	9.50×10^{-5}

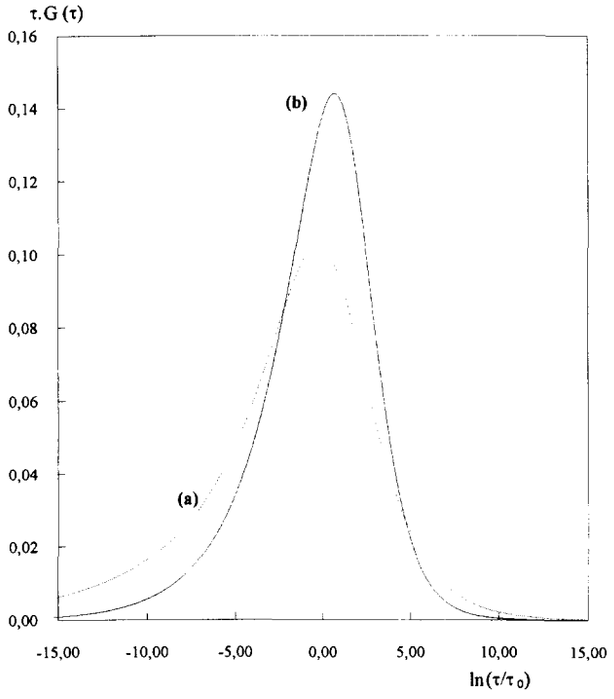

Figure 6 Distribution of relaxation times of PDMP obtained using: (a) the graphical method; (b) the LEVM6 program

Figure 4 Diagrams showing the change in the distribution of the relaxation times for: (a) $k = 0.00, 0.05, 0.10, 0.15, 0.20, 0.30, \ldots, 0.80$ ($h = 0.8$, $\delta = 1$, $\tau_0 = 10^{-5}$ s); (b) $h = 0.40, 0.45, 0.50, \ldots, 0.90$ ($k = 0.4$, $\delta = 1$, $\tau_0 = 10^{-5}$ s); (c) $\delta = 0.0, 0.2, \ldots, 2.0$ ($h = 0.8$, $k = 0.4$, $\tau_0 = 10^{-5}$ s)

Table 2 H–N parameters obtained for PDMP by using the LEVM6 program, compared with those obtained from the biparabolic model

Parameter	H–N model	Biparabolic model
ϵ_0	4.1879	4.1854
ϵ_∞	3.1879	3.2175
α	0.6128	0.7429
β	0.4707	0.2884
τ_0' (s)	9.44×10^{-5}	9.5×10^{-5}

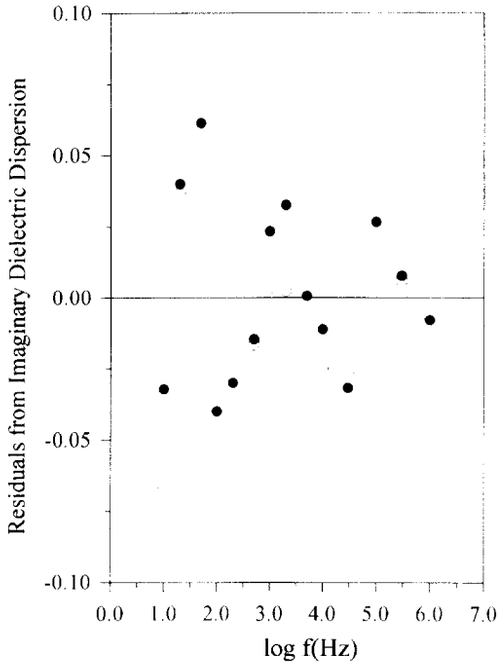

Figure 7 Plots of the imaginary residuals against log frequency for PDMP at 195°C: (●) the H–N model; (○) the biparabolic model

using the graphical method[22], while the second column gives the estimates obtained when using the LEVM6 program.

In *Figure 6* we can see the distribution relaxation times obtained by using both of the collections of parameters reported in *Table 1*. The δ' and τ_0' parameters are of the same order of magnitude in both cases, whereas the ϵ_0, ϵ_∞, h and k parameters are very sensitive to the method employed. The critical parameters are ϵ_0 and ϵ_∞, because in order to obtain the k and h parameters, the first of these is employed, respectively.

The relatively different values of the parameters obtained by both methods change the shape of the distribution function. The analysis of these functions indicates again that the most critical parameters for this function are h and k.

We can see from *Figure 6* that the distribution function obtained when using the method which involves the LEVM6 program has a higher maximum than the corresponding function obtained when using the graphical method, in accordance with our expectations (*Figure 4*).

This result suggests that the application of the LEVM6 program provides several important benefits in the analysis of the dielectric coefficients of polymers, as opposed to the original graphical analysis; one of these is the possibility of quantifying errors by means of the analysis of residuals, as in the method followed by Havriliak and Watts[24] which employed alternative statistical methods.

In this context, it is interesting to compare the results obtained by using the biparabolic model with those found when using the H–N equation (with the LEVM6 program), because according to equation (14) we can establish a relationship between the parameters of both models (see *Table 2*). An inspection of this table reveals that the most sensitive parameters are $\alpha = h$, and $\alpha\beta = k$. Although, on formal grounds, the asymptotic behaviour of both models is the same (equation (14)), a different set of values can be obtained for each model after fitting has been carried out. Moreover, in spite of the physical meaning of the biparabolic model in representing the experimental data, an analysis of the residuals of both equations in fitting the obtained values for PDMP (*Figure 7*) indicate that there are not significant advantages to be gained in using an extra parameter.

ACKNOWLEDGEMENT

The authors express their thanks to CICYT for financial support through Grant MAT-065/91.

REFERENCES

1 Havriliak, S. and Negami, S. *J. Polym. Sci. (C)* 1966, **14**, 99
2 Havriliak, S. and Negami, S. *Polymer* 1967, **8**, 161
3 Cole, K. and Cole, R. H. *J. Chem. Phys.* 1941, **9**, 341
4 Davidson, D. W. and Cole, R. H. *J. Chem. Phys.* 1951, **19**, 1484
5 Schonhals, A. and Schlosser, E. *Colloid Polym. Sci.* 1989, **267**, 125
6 Schonhals, A. and Schlosser, E. *Colloid Polym. Sci.* 1989, **267**, 133
7 Schonhals, A. and Schlosser, E. *Colloid Polym. Sci.* 1989, **267**, 963
8 Huet, C. *Ann. Ponts Chaussees* 1965, **VI**, 5
9 Ross Macdonald, J. 'Impedance Spectroscopy', Wiley, New York, 1987
10 Nonenmacher, T. F. in 'Lecture Notes in Physics' (Ed. J. Casas), Vol. 381, Springer, 1991, p. 309
11 Pérez J. *Acta Metall.* 1984, **12**, 2163
12 Decroix, J. Y., Piloz, A., Douillard, A., May, J. F. and Vallet, G. *Eur. Polym. J.* 1975, **11**, 625
13 Decroix, J. Y., Piloz, A. and May, J. F. *Eur. Polym. J.* 1976, **12**, 847
14 Pérez, J. *Rev. Phys. Appl.* 1986, **21**, 93
15 Pérez, J. *Rev. Phys. Appl.* 1988, **23**, 125
16 Johari, G. P. *Ann. N. Y. Acad. Sci.* 1976, **279**, 105
17 Ngai, K. L., Mashimo, S. and Fytas, G. *Macromolecules* 1988, **21**, 3030
18 Ngai, K. L., Rajagopal, A. K. and Teitler, S. *J. Chem. Phys.* 1988, **88**, 5086
19 Diaz Calleja, R., Riande, E. and Guzmán, J. *J. Polym. Sci. Polym. Phys. Edn* 1990, **28**, 1551
20 Titchmarsh, E. C. 'Introduction to the Theory of Fourier Integrals', Oxford University Press, Oxford, 1937
21 Böttcher, C. J. F. and Bordewijk, P. 'Theory of Electric Polarization', Elsevier, 1980, p. 523
22 Diaz Calleja, R., Devine, I., Gargallo, L. and Radic, D. *Polymer* 1994, **35**, 151
23 Sanchis, M. J., Díaz Calleja, R., Gargallo, L. and Radic, D. *Makromol. Chem. Rapid Commun.* 1994, **15**, 31
24 Havriliak Jr, S. and Watts, D. G. *Polymer* 1986, **27**, 1509